LMRS: An Integrated Lane Change Model with Relaxation and Synchronization

Ir. Wouter J. Schakel (corresponding author)
Department of Transport & Planning
Faculty of Civil Engineering and Geosciences
Delft University of Technology
Stevinweg 1, P.O. Box 5048, 2600 GA Delft, The Netherlands
phone +31 15 2784030
fax +31 15 2783179
e-mail w.j.schakel@tudelft.nl

Dr. Ir. Victor L. Knoop
Department of Transport & Planning
Faculty of Civil Engineering and Geosciences
Delft University of Technology
Stevinweg 1, P.O. Box 5048, 2600 GA Delft, The Netherlands
phone +31 15 2788413
fax +31 15 2783179
e-mail v.l.knoop@tudelft.nl

Prof. Dr. Ir. Bart van Arem
Department of Transport & Planning
Faculty of Civil Engineering and Geosciences
Stevinweg 1, P.O. Box 5048, 2600 GA Delft, The Netherlands
phone +31 15 2784874
fax +31 15 2783179
e-mail b.vanarem@tudelft.nl

Word Count	
Abstract	190
Main text	5796
Figures (4)	1000
Tables (2)	500
Total	**7486**

Submitted July 28th 2011

ABSTRACT

We propose a new lane change model that can be integrated with a car-following model to form a complete microscopic driver model. The aim of the model is to better resemble traffic at a macroscopic level, especially regarding the amount of traffic volume per lane, the traffic speeds at different lanes and the onset of congestion. The model takes a new approach where different lane change incentives are combined to determine a lane change desire. Included incentives are to follow a route, to gain speed and to keep right. Classification of lane changes is based on behavior which depends on the level of lane change desire. The integration with a car-following model is achieved by influencing car-following behavior for relaxation and synchronization, i.e. following vehicles in adjacent lanes. Other improvements of our model are trade-offs between different lane change incentives and the use of anticipation speed for the speed gain incentive. Although all these effects are captured, the lane change model has only 7 parameters. The model has been calibrated and validated using loop detector data, showing a very accurate representation of lane distribution and the onset of congestion.

INTRODUCTION

Microscopic simulation is often used to evaluate the effects of traffic measures and new technologies. The strength of microscopic simulation is the high level of detail and accuracy. This however generally comes at the expense of a high number of parameters. This makes calibration a cumbersome and difficult process. Microscopic traffic models generally have two main components, a longitudinal (or car-following) model and a lateral (or lane change) model. In some cases the lane change model uses the car-following model which constitutes an integrated model.

Much research has been performed into car-following resulting in many car-following models such as Gipps [1], Wiedemann [2], the optimal velocity model (OVM) [3], Tampère [4] and the Intelligent Driver Model (IDM) [5]. Lane change models have received less attention, especially the aspect of mandatory lane changes. For instance, Kesting et al. [6] and Laval et al. [7] only look at speed as an incentive to change lane. Gipps [8] was one of the first to formulate a model for lane changes that was intended to be integrated with a car-following model. Many lane change models since then make a distinction between mandatory and discretionary lane changes. A problem with these models is that there is no trade-off between them. Toledo et al. [9] recognized this and formulated a lane change model with incentives combined.

For most lane change models it holds that gap-acceptance is either a simple function of distance and speed difference, or is based on a car-following model to determine resulting deceleration. The first class of gap-acceptance models fails to include car-following dynamics while for the latter class it is assumed that drivers accept smaller gaps through a larger acceptable deceleration. However, in reality, drivers will mostly apply small decelerations and will accept smaller time headways for some time, as is shown empirically for merging traffic [10]. This phenomenon is known as relaxation [11]-[13].

Another important aspect of lane changing is lane change preparation, sometimes referred to as the tactical stage [6], in which drivers may adapt their speed, align with a gap and in which another driver may create a gap. We will refer to this lane change preparation as synchronization, as drivers synchronize with an adjacent lane. Only little literature is available describing models for synchronization and relaxation [14]-[17].

In regard of this brief overview of lane change models there is a need for a new lane change model. The main goal is the achievement of a good resemblance with reality at lane-level regarding the amount of traffic on each lane (lane distribution) and the speed driven on each lane (lane speed). The model should be applicable for various road layouts and various levels of traffic density. To achieve this, multiple lane change incentives need to be included. A secondary but still important goal is to resemble traffic dynamics including the onset and progression of congestion. For this we include relaxation and synchronization into our model. A final requirement is that it should be possible to calibrate the model. For this the complexity and number of parameters should be limited. To our knowledge, there is no lane change model that fulfills these requirements.

In this paper, we introduce the Lane change Model with Relaxation and Synchronization (LMRS) that includes both mentioned phenomena. We will discuss the integration with a car-following model using an adapted version of the Intelligent Driver Model (IDM) [5]. LMRS can be used with any car-following model that calculates vehicle acceleration. In this paper we assume some parameters to be part of the car-following model, but this is not a strict requirement. The integration with the car-following model is twofold. First, the car-following model is used for gap-acceptance, where different headways apply due to relaxation. Second, synchronization triggers car-following to vehicles in adjacent lanes as lane change preparation.

Most lane change models classify lane changes by the reason for which they are performed, e.g. mandatory, discretionary, courtesy etc. [18]. We classify lane changes by the way in which they are prepared and performed. We call this a lane change process and different processes are performed for different levels of desire. Note that in the remainder of this paper 'desire' refers to lane change desire and 'process' refers to lane change process. Throughout this paper we will drop subscripts where possible for the sake of readability. We will also drop (*t*) for time dependent quantities where possible; a reaction time is not included in the model.

This paper is structured as follows. First, the lane change desire and accompanying processes are explained. The next section will elaborate on the determination of lane change incentives. The integration with a car-following model is discussed in the next section, followed with a section about calibration and validation. Finally the conclusions are given.

LANE CHANGE DESIRE AND PROCESS

This section will introduce the main mechanism of LMRS which is structured around lane change desire. Before explaining our model we show a list of frequent symbols throughout this paper.

$\dot{v}$	acceleration as determined by car-following model
d	lane change desire
s	net distance headway
T	net time headway
k, i, j	pertaining specific, current and target lane respectively
v	speed
x	distance
Δ	whether lane change is applicable (1) or not (0) for a specific incentive

The desire to change from lane *i* to lane *j* that arises from the different incentives is combined into a single desire.

$$d^{ij} = d_r^{ij} + \theta_v^{ij} \cdot \left(d_s^{ij} + d_b^{ij} \right) \tag{1}$$

We have a desire to follow a route (d_r), to gain speed (d_s) and to keep right (d_b), where the subscript *b* stands for bias to a particular side. The latter two are included with θ_v which is the level at which voluntary (discretionary) incentives are included. In the next section it is explained how these quantities are determined. Desire is meaningful between -1 and 1 where negative values indicate that a lane change is not desired (i.e. to stay or to change in the other direction). Values outside of the meaningful range may exist as incentives are added.

The total desire determines the behavior of drivers. Classification of lane changes is based on this behavior. We distinguish: Free Lane Changes (FLC), Synchronized Lane Changes (SLC) and Cooperative Lane Changes (CLC). To this end we split the desire range into four sub-ranges using three thresholds relating to the processes:

$$0 < d_{free} < d_{sync} < d_{coop} < 1 \tag{2}$$

Desire as calculated with equation (1) falls within a particular range with an accompanying process. Figure 1 gives an overview of the variation of lane change behaviour between processes. For little desire, no lane change will be performed. For a somewhat larger desire, FLC is performed requiring no preparation whatsoever. In SLC and CLC a potential lane changer is willing to synchronize speed with the target lane. This is achieved by following a vehicle in that lane. Concurrently this will align the vehicle with a gap (if there is a gap); this is thus a simple gap-searching model. In CLC, the potential follower will additionally start to create a gap by following the potential lane changer. This behaviour is also called synchronization and may be triggered for several reasons such as the use of a turn indicator or the lateral in-lane position. An important reason is however the synchronization of the potential lane changer itself. From this behaviour a driver may deduce that an adjacent vehicle wants to change lane. Throughout this paper we assume that drivers are able to note whether the lane change desire of another driver is smaller or larger than d_{coop}. Empirical evidence that drivers are willing to create a gap, at least at an on-ramp, can be found in [10] where no merging vehicle is overtaken by multiple vehicles.

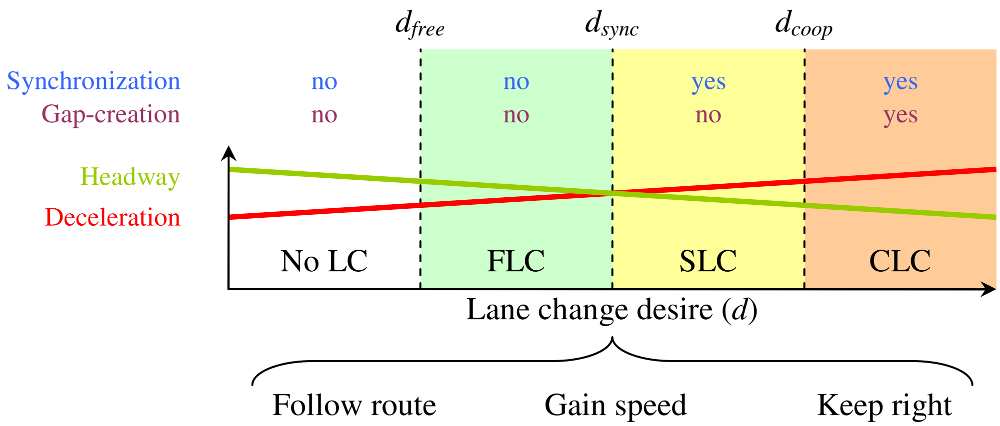

FIGURE 1 Overview of LMRS. Lane change desire is based on three incentives. Lane change behavior, including the accepted headway and deceleration for a lane change, varies depending on the level of lane change desire.

Besides the synchronization there are also desire dependant differences in the accepted headway and deceleration that would arise if a lane change is initiated. For higher desire drivers are willing to accept smaller headways and to decelerate more. Note however that the maximum deceleration will be smaller in our model than in most existing lane change models such as MOBIL [6] where a value of 4 m/s^2 is used, which is rather high. This is achieved by allowing for relaxation and synchronization.

Desire to change both left and right is determined. Also the possibility (gap-acceptance) to both sides is assessed. The lane change with highest desire will be performed if possible and desired ($d \geq d_{free}$). If the lane change is not possible, lane change preparation (SLC and CLC) may be performed.

LANE CHANGE INCENTIVES

This section will elaborate on the quantities of equation (1) in detail. In this paper we assume asymmetric traffic rules, where drivers have to keep right and may only overtake on the left. Consequently a speed advantage is only considered to the left lane and in certain circumstances there may be a bias to the right. In our model we will not explicitly prevent vehicles from overtaking on the right, as this often happens in reality despite the prohibition. Note however that a speed advantage is not actively considered in the right lane. Our model can be easily adapted for symmetric or left-hand traffic rules.

Several parameters will be introduced in this and the next section. For an overview of all parameters the reader is referred to table 1 on page 13.

Anticipation Speed

The voluntary incentives as described in the following sub-sections use anticipation speed. This section will first elaborate on how this quantity is determined using the following quantity definitions:

v_{ant}	Anticipation speed, or the considered speed at a lane
v_{lim}	The speed limit
v_{max}	Maximum vehicle speed
v_{des}	Desired speed
v_{lead}	The actual speed of an (adjacent) leader
$\tilde{v}_{lead}$	The considered speed of an (adjacent) leader given the headway
x_0	Anticipation distance
δ	Speed limit adherence factor

The anticipation speed is intended to represent to which extent drivers take account of downstream vehicles. The further away the vehicle is, the less influence the vehicle has. The slower a vehicle is, the more it may reduce the anticipation speed. The anticipation speed v_{ant} on a lane is a function of v_{lim}, v_{max} and v_{lead} where v_{lead} is considered for several leading vehicles (potentially) on the assessed lane. The quantities v_{lim} and v_{max} are combined into a desired speed for lane k as:

$$v_{des}^{k} = \min\left(\delta \cdot v_{lim}^{k}, v_{max}\right) \quad (3)$$

This expression includes a level of adherence δ with regard to the speed limit. For $\delta > 1$ this results in speeding and for $\delta < 1$ this results in the opposite.

The speed of any leading vehicle v_{lead}, may be of influence on the anticipation speed. Clearly, a slow leader lowers the anticipation speed. However, if this leader is very far away, the vehicle is not considered at all. We have $\tilde{v}_{lead}\left(s=0\right)=v_{lead}$ where the vehicle is fully considered and $\tilde{v}_{lead}\left(s=x_0\right)=v_{des}$ where the vehicle is completely ignored. We use the anticipation distance x_0 which is also a parameter for the route incentive as described in a next sub-section. For intermediate headways we interpolate linearly giving:

$$\tilde{v}_{lead} = \left(1 - \frac{s}{x_0}\right) \cdot v_{lead} + \frac{s}{x_0} \cdot v_{des} \tag{4}$$

The anticipated speed on lane k is given by:

$$v_{ant}^{k} = \min\left(v_{des}^{k}, \min_{m \in M_k}\left(\tilde{v}_{lead}^{m}\right)\right) \tag{5}$$

where all leading vehicles from the set M_k are taken into account. This set is lane dependant and entails vehicles with a headway shorter than x_0. The set M_k by definition entails all vehicles on lane k, all vehicles on lane k-1 (left) with $d^{k-1,k} \geq d_{coop}$ and all vehicles on lane k+1 (right) with $d^{k+1,k} \geq d_{coop}$. Vehicles with $d^{k,j} \geq d_{coop}$ if $k = i$ (i being the current and j being the considered lane) are however never considered. In other words; all vehicles on, or potentially on, a certain lane are considered for the anticipation speed on that lane. When assessing the anticipation speed on an adjacent lane, potential lane changers from the current lane are excluded. This exclusion is put in place to prevent situations where large speed differences between lanes are persistently maintained as drivers anticipate a slow speed on the faster lane due to other slow vehicles with a desire towards that lane.

Speed Incentive

We assume that drivers may desire to change lane in order to increase their speed. We also assume that drivers are particularly anticipative when assessing the speed on a lane, i.e. if possible flying takeovers are performed where no speed is actually lost. Hence, to assess the desire we use the anticipation speed. Regarding the speed incentive the following assumptions are made:

- A full desire is experienced for a speed gain of v_{gain}
- Desire is linearly related to speed gain
- Drivers ignore a possible speed gain towards the right lane at high speeds ($v_{ant} > v_{crit}$)
- Desire to change lane is reduced while accelerating

For the latter assumption we introduce a_{gain} as a reduction factor on desire. It is defined as:

$$a_{gain} = \frac{a - \max\left(\dot{v}, 0\right)}{a} \tag{6}$$

where a is the maximum acceleration from the car-following model. We also have Δ_s which defines whether a lane change is possible and allowed ($\Delta_s = 1$) or not ($\Delta_s = 0$). Desire from the speed incentive is now defined as:

$$d_s^{i,i-1} = \begin{cases} a_{gain} \dfrac{v_{ant}^{i-1} - v_{ant}^{i}}{v_{gain}}, & \Delta_s^{i,i-1} = 1 \\ 0, & \Delta_s^{i,i-1} = 0 \end{cases}$$

$$d_s^{i,i+1} = \begin{cases} a_{gain} \dfrac{\min\left(v_{ant}^{i+1} - v_{ant}^{i}, 0\right)}{v_{gain}}, & \Delta_s^{i,i+1} = 1 \text{ and } v_{ant}^{i} > v_{crit} \\ a_{gain} \dfrac{v_{ant}^{i+1} - v_{ant}^{i}}{v_{gain}}, & \Delta_s^{i,i+1} = 1 \text{ and } v_{ant}^{i} \le v_{crit} \\ 0, & \Delta_s^{i,i+1} = 0 \end{cases} \quad (7)$$

where *i*-1 and *i*+1 are the left and right adjacent lanes respectively. Note that a speed *loss* is always considered towards the right lane to be balanced with other incentives.

As the speed incentive is based on anticipation speed, it is also based on adjacent vehicles that have $d > d_{coop}$. In case these vehicles lower the anticipation speed, a driver may be triggered to perform a courtesy lane change. These are lane changes that are performed to create a gap for another vehicle.

Route Incentive

If the current lane will not allow a route to be followed, lane change desire arises. This may be because the lane ends or because the lane will turn into another direction. For these situations we make the following assumptions:

- At relatively high speeds, the remaining time per required lane change determines desire. This is different from existing models such as Gipps [8] and the lane change model in FOSIM [19] where desire is based on distance. Desire starts at a remaining time of t_0 per lane change.
- At relatively low speeds, the remaining distance becomes dominant in determining desire. Desire starts at a remaining distance of x_0 per lane change.
- Desire increases linearly towards full desire for decreasing time or distance.
- Desire from the route incentive exists even if the lane change is (currently) not possible.

The latter assumption may trigger synchronisation upstream of an actual merge location, which is common practice at merge locations. In order to determine desire for the route incentive we define x_r^k as the remaining distance, $t_r^k = x_r^k/v$ as the remaining time given current speed v and n_r^k as the number of required lane changes, all for lane k. Desire is now determined as:

$$d_r^k = \max\left(1 - \frac{x_r^k}{n_r^k \cdot x_0}, 1 - \frac{t_r^k}{n_r^k \cdot t_0}, 0\right) \quad (8)$$

which defines the desire to *leave* lane *k*. To derive the desire to either the left or right lane we compare the desire on the target and current lane. If the desire to leave the target lane is smaller than the desire to leave the current lane, we use the desire to leave the current lane. The other way around we use the negative value of the desire to leave the target lane, i.e. the lane change is undesired with the amount to leave the target lane. This is defined as:

$$d_r^{ij} = \begin{cases} d_r^i, & \Delta_r^j = 1 \text{ and } d_r^i > d_r^j \\ 0, & \Delta_r^j = 1 \text{ and } d_r^i = d_r^j \\ -d_r^j, & \Delta_r^j = 1 \text{ and } d_r^i < d_r^j \\ -\infty, & \Delta_r^j = 0 \end{cases} \qquad (9)$$

where $\Delta_r = 1$ indicates that the route can still be followed on the target lane.

Keep-right Incentive

A simple incentive in accordance with the 'keep right if possible' traffic rule that is implemented in many models is a constant bias to the right lane, such as for example in MOBIL [6]. Indeed drivers will be inclined to change to the right. However, the phrase 'if possible' is stretched if drivers are forced to drive somewhat slower than their desired speed. In fact, the slugs and rabbits theory of Daganzo [20] predicts more traffic on the left lane for typical percentages of slow traffic. However, if there is no slow traffic on the right lane for some considerable distance, a driver would at some point change right. Here, we only need to compensate the lane change threshold d_{free} whenever a vehicle anticipates an unhindered speed on the right lane.

Another influence on right-keeping behaviour is a downstream turn. Drivers are not willing to change right if that lane will turn into a wrong direction, even in light traffic conditions. If a driver is within the region defined by t_0, it will experience a slight negative desire to change right. In that case we assume that drivers do not obey the traffic rule. In short, drivers will obey the keep-right rule only if the situation on the right lane is not worse with respect to speed and route. This is expressed as:

$$d_b^{i,i-1} = 0$$
$$d_b^{i,i+1} = \begin{cases} d_{free}, & v_{ant}^{i+1} = v_{des} \text{ and } d_r^{i,i+1} \geq 0 \\ 0, & \text{otherwise} \end{cases} \qquad (10)$$

Consideration of Incentives

Depending on the urgency of mandatory lane changes, drivers may (partially) ignore voluntary lane change incentives. We therefore use θ_v which is the level at which voluntary desire is included in the decision. It depends on the level of (negative) mandatory desire, as this may become dominant. For sake of argument we will use total voluntary desire $d_v = d_s+d_b$. If both voluntary and mandatory desire are either negative or positive ($d_r \cdot d_v \geq 0$), voluntary desire is fully included as it coincides with mandatory desire. However, if voluntary desire is conflicting with mandatory desire ($d_r \cdot d_v < 0$), the voluntary desire is only partially included. For strong mandatory desire, negative or positive ($|d_r| > d_{coop}$), voluntary desire is ignored. For mild mandatory desire ($|d_r| < d_{sync}$), voluntary desire is fully included. In between, the consideration of voluntary desire is linearly interpolated. This is expressed as:

$$\theta_v^{ij} = \begin{cases} 0, & d_r^{ij} \cdot d_v^{ij} < 0 \quad \text{and} \quad \left| d_r^{ij} \right| \ge d_{coop} \\ \dfrac{d_{coop} - \left| d_r^{ij} \right|}{d_{coop} - d_{sync}}, & d_r^{ij} \cdot d_v^{ij} < 0 \quad \text{and} \quad d_{sync} < \left| d_r^{ij} \right| < d_{coop} \\ 1, & \underbrace{d_r^{ij} \cdot d_v^{ij} \ge 0}_{\text{conflict/coincide}} \quad \text{or} \quad \underbrace{\left| d_r^{ij} \right| \le d_{sync}}_{\text{mandatory dominance}} \end{cases} \tag{11}$$

INTEGRATION WITH A CAR-FOLLOWING MODEL

We have presented how the lane change model determines desire to change lane. In this section we will discuss the integration with a car-following model related to gap-acceptance and relaxation, gap-creation and synchronization and we will discuss the used car-following model.

Gap-acceptance and relaxation

A gap is accepted or rejected based on the resulting deceleration that follows from the car-following model. Gaps that result in deceleration that is too large, are rejected as they are unsafe, uncomfortable or impolite. This is similar as in MOBIL [6], except that the applicable headway is changed. The gap is accepted if both the lane changer (*c*) and the new follower (*f*) will have an acceleration that is larger than some safe deceleration threshold $-b^c$ as in:

$$\dot{v}^g \ge -b^c \cdot d^{ij,c} \tag{12}$$

with $g \in \{c, f\}$. For clarity we explicitly mention to which vehicle the parameters pertain. The applicable headway for both the lane changer and the new follower is given by:

$$T^g\left(d^{ij,c}\right) = \min\left(T^g(t), \left\langle d^{ij,c} \right\rangle \cdot T_{min}^g + \left(1 - \left\langle d^{ij,c} \right\rangle\right) \cdot T_{max}^g\right) \tag{13}$$

where,

$T^g(t)$	Current following time headway of vehicle g including previous relaxation
T_{max}^g	Regular following time headway of vehicle g
T_{min}^g	Minimum following time headway at maximum desire of vehicle g
$\left\langle d^{ij,c} \right\rangle$	Lane change desire of vehicle c limited between 0 and 1

From equations (12) and (13) one can see that for larger desire, larger decelerations and shorter headways are accepted. If the lane change is actually initiated, both vehicle *c* and *f* should update the value for $T^g(t)$ to the value of $T^g(d^{ij,c})$. The relaxation of the headway value is assumed exponential with relaxation time τ. In a numerical update scheme with time step Δt we can use:

$$T(t) = T(t - \Delta t) + \left\{T_{max} - T(t - \Delta t)\right\} \frac{\tau}{\Delta t} \tag{14}$$

Synchronization and Gap-creation

When lane change desire is above the synchronization threshold, drivers will start to synchronize their speed with the leader on the target lane by applying the car-following model resulting in

$\dot{v}_{sync}^{ij}$. Drivers will apply a maximum deceleration of b which is considered a both comfortable and safe deceleration. The maximum deceleration for speed synchronization is given by:

$$\dot{v}_{sync}^{ij} > -b \tag{15}$$

If an adjacent leader wishes to change lane with a desire above the cooperation threshold, a gap will be created. Gap creation is very similar to synchronization and we again apply the car-following model with a limited deceleration as in equation (15).

Used car-following model

We will use a slightly adapted version of the Intelligent Driver Model (IDM) by Treiber et al. [5]. The acceleration is calculated with

$$\dot{v} = a \cdot \min\left(1 - \left(\frac{v}{v_{des}}\right)^4, 1 - \left(\frac{s^*}{s}\right)^2\right) \tag{16}$$

and

$$s^* = s_0 + v \cdot T + \frac{v \cdot \Delta v}{2\sqrt{a \cdot b}} \tag{17}$$

where s_0 is the stopping distance, Δv is the approaching rate to the leader, s is the net distance headway and s^* is the dynamic desired headway. The adapted model is referred to as IDM+ and differs from the IDM solely by the minimization over, instead of addition of, components in equation (16). This adaption has been made to increase the capacity to more realistic values, as well as having $\dot{v} = 0$ for $v = v_{des}$ and $s = s^*$. For further details, see Schakel et al. [21].

Car-following models are usually designed for in-lane dynamics. In multi-lane traffic, headways and speed difference between lanes have a wider range of values. In the IDM negative values of either s or s^* have the same effect as positive values because of the power of two. Negative headways occur for adjacent vehicles and a negative dynamic desired headway may occur for large negative values of Δv. We will therefore use these boundary conditions:

$$\begin{aligned} s &> 0 \\ s^* &\geq 0 \end{aligned} \tag{18}$$

CALIBRATION AND VALIDATION

In this section we describe the model calibration and validation. We discuss the model implementation, the calibration setup and the data. In the end the results are shown.

Model Implementation

Although the LMRS has been presented in very small detail, the precise implementation can still have influence on model results. In this section we briefly present our implementation. The procedure in the box below should be performed for each driver at each time step. The minimum acceleration based on all applicable leaders should be used. We have used a lane change duration of 3s (from FOSIM [19]) during which a virtual and temporary vehicle is placed on the target lane to prevent other lane changes towards the same location. Over the first 100m of the network, lane changes are never performed as upstream vehicles that influence such a lane change may not yet be generated. We have used Δt = 0.5s (from FOSIM [19]) as a balance between short running times and modeling precision. On a dual CPU 2.8 GHz this results in running times in the order of 10-50 seconds per modeled hour depending on the level of congestion (i.e. number of vehicles ranging from 150 to 600).

Steps	Equation(s)
While not changing lane	
1. relax headway	(14)
2. calculate route desire	(8)-(9)
3. calculate anticipated speeds	(3)-(5)
4. calculate speed desire	(6)-(7)
5. calculate keep-right desire	(10)
6. combine desires	(11), (1)
7. gap-acceptance	(12)-(13)
8. make lane change decision (see page 5)	
9. follow leader	(16)-(18)
10. if applicable, synchronize	(16)-(18), (15)
11. if applicable, create gap	(16)-(18), (15)
During lane change	
1. follow old and new leader	(16)-(18)

Calibration Setup

We apply the LMRS in combination with the IDM+. The full model has 20 parameters which are too many to calibrate as this will take very long and because a solution will be difficult to find as there are many degrees of freedom. We alleviate this problem in two ways. Not all parameters will be calibrated as some are fairly well known. Two parameters, d_{sync} and d_{coop}, will be related to d_{free}, reducing the number of parameters pertaining to lane changes from 9 to 7. Second, two calibration scenarios will be used. In the first scenario the model will be calibrated to free flow conditions, calibrating parameters that can be determined in free flow. In the second scenario the model will be calibrated to congested conditions, calibrating the remaining parameters. This approach follows the reasoning as presented by Ossen et al. [22]. The benefits of this approach are that each iteration of the calibration procedure involves less model runs, the calibration will converge in less iterations and the short duration of free flow runs.

An overview of all model parameters is given in table 1. We apply two classes being passenger cars and trucks. Most parameters are equal between classes except for the acceleration (a), vehicle length (l) and desired speed. For cars we assume the desired speed is given by driver preference $\delta_{car} = N(v_{des,car}, \sigma_{car})/v_{lim}$ where $N(v_{des,car}, \sigma_{car})$ is a Gaussian distribution with mean $v_{des,car}$ and standard deviation σ_{car}. For trucks we assume the desired speed is given by the maximum vehicle speed $v_{max,truck} = N(v_{des,truck}, \sigma_{truck})$.

TABLE 1 Overview of Model Parameters.

Symbol	Initial or assumed value	Calibration[a]	Calibrated value	Remarks[b]
		Regular car-following parameters		
a_{truck}	0.4 m/s^2	fixed		Taken from FOSIM [19].
a_{car}	1.0 m/s^2	congestion	1.25 m/s^2	In [5] a value of 0.73 was found. This however pertains to mixed traffic. For cars we start somewhat higher.
b	1.67 m/s^2	congestion	2.09 m/s^2	In [5] a value of 1.67 was found which we will use.
T_{max}	1.2 s	congestion	1.2 s	On the left lane of the two-lane section of our network we find maintainable flows around 2400 veh/h. From this we calculate a value of 1.2s at 90 km/h.
s_0	3 m	fixed		This value is based on the length of cars and a jam density of about 140 pce/km.
$v_{des,car}$	123.7 km/h	free flow	123.7 km/h	We fitted a cumulative Gaussian distribution to the average speeds in free flow on the middle and the left lane using the fractions of traffic on these lanes. We added 5% to the resulting fit as this approach gives a lower limit to desired speed.
σ_{car}	8.3 km/h	free flow	12.0 km/h	See $v_{des,car}$.
$v_{des,truck}$	85 km/h	fixed		Taken from FOSIM [19].
σ_{truck}	2.5 km/h	fixed		It is assumed that the majority of trucks has a desired speed between 80 and 90 km/h.
l_{car}	4 m	fixed		Estimated using helicopter data from [23].
l_{truck}	15 m	fixed		Estimated using helicopter data from [23].
		Lane change related parameters		
T_{min}	0.7 s	congestion	0.56 s	Based on [10] we assume an average minimum headway of 0.7s.
τ	20 s	congestion	25 s	Some studies ([11]-[13], [16]) estimate values between 20-30s. Due to our exponential relaxation we assume a value at the lower end.
x_0	300 m	free flow	295 m	Based on the last traffic signs indicating a lane-drop.
t_0	67 s	free flow	43 s	In [8] a value of 50s resembles driver behavior. We set this equal to $t_0 \cdot (1-d_{free})$, where lane changes start.
d_{free}	0.25	free flow	0.365	We start with four equal desire ranges.
d_{sync}	0.50	related	0.577	The range beyond d_{free} is equally divided, $d_{sync} = d_{free} + ⅓(1-d_{free})$
d_{coop}	0.75	related	0.788	The range beyond d_{free} is equally divided, $d_{coop} = d_{free} + ⅔(1-d_{free})$
v_{gain}	70 km/h	free flow	69.6 km/h	Based on d_{free} and speed differences between lanes in the order of 15-20 km/h on our road stretch we start with 70 km/h.
v_{crit}	60 km/h	fixed		Estimated on plots of speed vs. lane fraction where in the range around 60 km/h, fractions tend to become more equal.

[a] Whether a value is fixed, related to another parameter or calibrated in a scenario.
[b] Describes how initial or assumed values have been determined. Values were additionally determined with a few initial runs of the model.

As mentioned, we use two calibration scenarios. Parameter values found in the free flow scenario which is performed first, are used in the congestion scenario. The error measure ε which should be minimized is based on a comparison of real and virtual detector data. In free flow we use:

$$\varepsilon_{free} = \sqrt{\frac{\sum_{n=1}^{N}\left(\left(\sum_{t=1}^{H} q_{n,t}^{real} - \sum_{t=1}^{H} q_{n,t}^{sim}\right)^2\right)}{N}} + 25 \cdot \sqrt{\frac{\sum_{n=1}^{N}\left(\left(\frac{H}{\sum_{t=1}^{H}\frac{1}{v_{n,t}^{real}}} - \frac{H}{\sum_{t=1}^{H}\frac{1}{v_{n,t}^{sim}}}\right)^2\right)}{N}} + m \quad (19)$$

where $t = 1 \ldots H$ is the considered time period, $n = 1 \ldots N$ are the considered detectors, q is a 1-minute flow count, v is the arithmetic mean speed of all vehicles within a minute and m is the number of deleted vehicles in simulation. The first part of equation (19) is the root mean squared error (RMSE) of hourly flow (as $H = 60$) of all detectors. The second part of equation (19) is the RMSE of the harmonic mean of speed measurements. We include the RMSE relating to speed with a factor of 25 meaning that an error of 25 veh/h is equal to an error of 1 km/h. Finally we include the number of deleted vehicles as, depending on the parameter values, drivers in the model may not be able to change lane before they have to. This is included to keep the number of deleted vehicles small.

For the congestion scenario we will use:

$$\varepsilon_{cong} = \sqrt{\frac{\sum_{n=1}^{N}\sum_{t=1}^{H}\left(60 \cdot \left(q_{n,t}^{real} - q_{n,t}^{sim}\right)\right)^2}{N \cdot H}} + 25 \cdot \sqrt{\frac{\sum_{n=1}^{N}\sum_{t=1}^{H}\left(v_{n,t}^{real} - v_{n,t}^{sim}\right)^2}{N \cdot H}} + m \quad (20)$$

which is similar to (19). Minute measurements are however not aggregated in order to capture the dynamics of congestion. For an equal comparison between flow and speed, the minute flows are calculated to hourly flows.

To find the optimal parameter values, we will use the calibration algorithm as presented below. We start with a large search space which is incrementally reduced in the second step. As soon as the search space is smaller than 0.1% of the parameter values, the algorithm stops. This method is unable to change the sign of a parameter, which is not a problem for our parameters.

<u>Optimization algorithm</u>

0. Start with x as the initial values of the parameters. Set $f = \{0.8, 1.25\}$.
1. For each parameter, look at two new points with a value which is a factor of $f(1)$ and $f(2)$ of the value in x.
    a. If a better point was found, set x at the best point. Redo step 1.
    b. If no better point was found, go to step 2.
2. Reduce the size of f by ⅔rd; $f(2) = 1+⅔\cdot(f(2)-1)$ and $f(1) = 1 / f(2)$.
    a. If $f(2) > 1.001$, redo step 1.
    b. If $f(2) \leq 1.001$, stop.

To cope with the stochastic nature of the model, each error is an average error of 5 model runs with different random seeds. A higher number of runs would give more certainty, but would also increase running times. Each simulation starts 10 minutes before the applicable period in order to fill the network.

Calibration and Validation Data

We calibrate our model using detector data on a section of the A20 freeway near Rotterdam in the Netherlands as in figure 2. The speed limit is 120 km/h. This section has a few on- and off-ramps and a lane drop, furthermore it has closely spaced detectors (300-500m). This data is to widely spaced to detect actual lane changes. However, the main purpose of our model is to accurately represent lane distributions, lane specific speeds and the onset and progression of congestion. These phenomena can be found in detector data, and the calibration is successful if these characteristics can be reproduced in simulation.

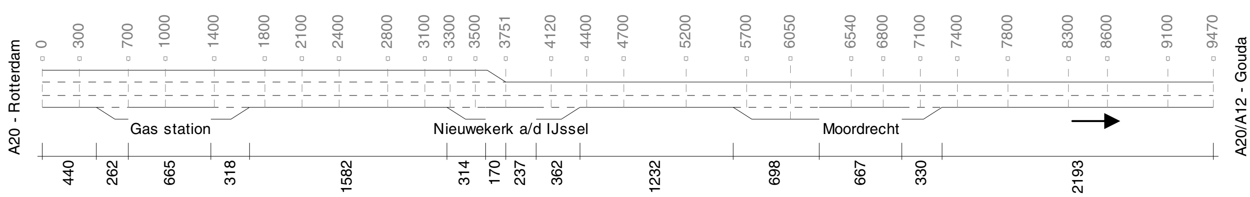

FIGURE 2 A20 network with distances and detector locations in meters.

Congestion on the A20 towards Gouda is often initiated by spillback from the off-ramp Moordrecht. For calibration we require that the traffic state on the network is not influenced by external disturbances. A detector on the off-ramp Moordrecht (not shown in figure 2) was used to find days where congestion started due to the lane-drop and on-ramp Nieuwekerk a/d IJssel and remained unaffected by the off-ramp for a considerable period. Two days were selected; Monday June 8th 2009 and Thursday June 25th 2009. The first day was used for calibration for free flow (5:15 – 6:15 AM) and congestion (6:00 – 7:00 AM) while the latter day was used for validation for free flow (5:30 – 6:30 AM) and congestion (6:15 – 7:15 AM). Truck percentages were very similar at 11.0% and 10.6% respectively.

Inflow into our model is based on detector data aggregated over one minute. During each minute, the vehicles are uniformly distributed. The number of vehicles to be generated on the on-ramps has been determined by subtracting the downstream flow from the upstream flow. This method may result in negative flows, which are solved by moving some vehicles earlier in time as this maintains the peaks in traffic demand.

Detector data was also used to estimate an origin-destination pattern, assuming a constant pattern over the simulated period. For each off-ramp, split fractions were determined. These were then used to assign probabilities of traffic from each origin towards the destinations taking consecutive split fractions into account. As the gas station is rather close to the beginning of the network, traffic towards the gas-station is only generated on the right and middle lane. Trucks are only generated on the right lane and on-ramps. The percentage of trucks was estimated using class specific traffic counts on the A20 upstream of our network. These traffic counts were aggregated per month, but separated per weekday.

Only detectors from x = 1400 till x = 7400 are considered for the error measure to allow traffic to settle and as downstream of on-ramp Moordrecht speeds may be influenced by a narrow bridge and road curvature.

Results

In table 1 the calibrated parameter values are given. Some parameters have not or hardly changed from the initial value. In general, these parameters have a range that may result in a more or less equal fit to data for as long as other parameters also change within such a range. Substantial changes from the initial values are found for a_{car}, b, σ_{car}, T_{min}, τ, t_0 and d_{free}. However, once these parameters received a few course adjustments at the beginning of the calibration, again a range of values can result in a more or less equal fit.

One remarkable observation from the parameter values is that drivers are apparently willing to change lane for a speed gain of $d_{free} \cdot v_{gain} \approx 25$ km/h or higher. We suspect that this rather large value is not only a minimum speed gain, but simultaneously an adjustment of speed at both the origin and target lane. For instance, a bounded driver on the right lane driving at 80 km/h, with a desired speed of 95 km/h, is willing to overtake its leader by temporarily driving 105 km/h in order not to holdup traffic on the left lane. The interpretation for v_{des} is thus a combination of desired speed and the speed at which drivers are willing to overtake. Such speed adaptation is however not explicitly modeled.

Another observation is that drivers look about 300m (x_0) ahead on the right lane and will not keep right if there is any slower vehicle within this range. This may appear to be a rather long range. The value may however result from the 3-lane section, where traffic on the middle lane will not feel inclined to keep-right as they can still be overtaken. Also, some drivers may have little to no attention for the keep-right rule.

In figure 3 calibrated lane fractions of the first run are shown related to the density at a cross-section with detectors. Lane fraction is the flow on a lane divided by the flow over all lanes. The density k_{road} is calculated as the flow over all lanes divided by the harmonic mean of the speeds on all lanes. The model is able to represent the relation between the density and the amount of traffic that can be found at different lanes. Furthermore we can see that between x = 2400 and x = 3500 the amount of traffic on the left lane reduces as it will we dropped at x = 3751. Consequently the amount of traffic on the middle lane increases while the amount of traffic on the right lane hardly changes. At x = 5200 there is more traffic on the right lane than at x = 3751. This is due to off-ramp Moordrecht as well as traffic moving away from the busy left lane due to the upstream lane drop.

Calibrated speeds of the first run are shown at a 3-lane cross-section and a 2-lane cross-section. There are clear differences between lanes, and speeds appear to drop linearly for increasing density (in free flow). The model is able to represent both phenomena. Runs 2 till 5 show similar results as run 1 with regard to lane fractions and lane speeds.

The results of the congestion scenario are presented in space-time-speed plots as these allow for good recognition of congestion patterns. These figures were created using the Adaptive Smoothing Method [24]. In figure 4 we can see that the calibration runs are able to produce comparable congestion with reality. There are however differences between congestion patterns, showing the influence of stochastic input. Similar plots were created for the validation day. Although there was mild congestion in reality, none of the 5 model runs showed congestion, although there are a lot of drops in speed, none of which actually trigger congestion. These drops in speed indicate that congestion could arise with only little changes in input or parameter values.

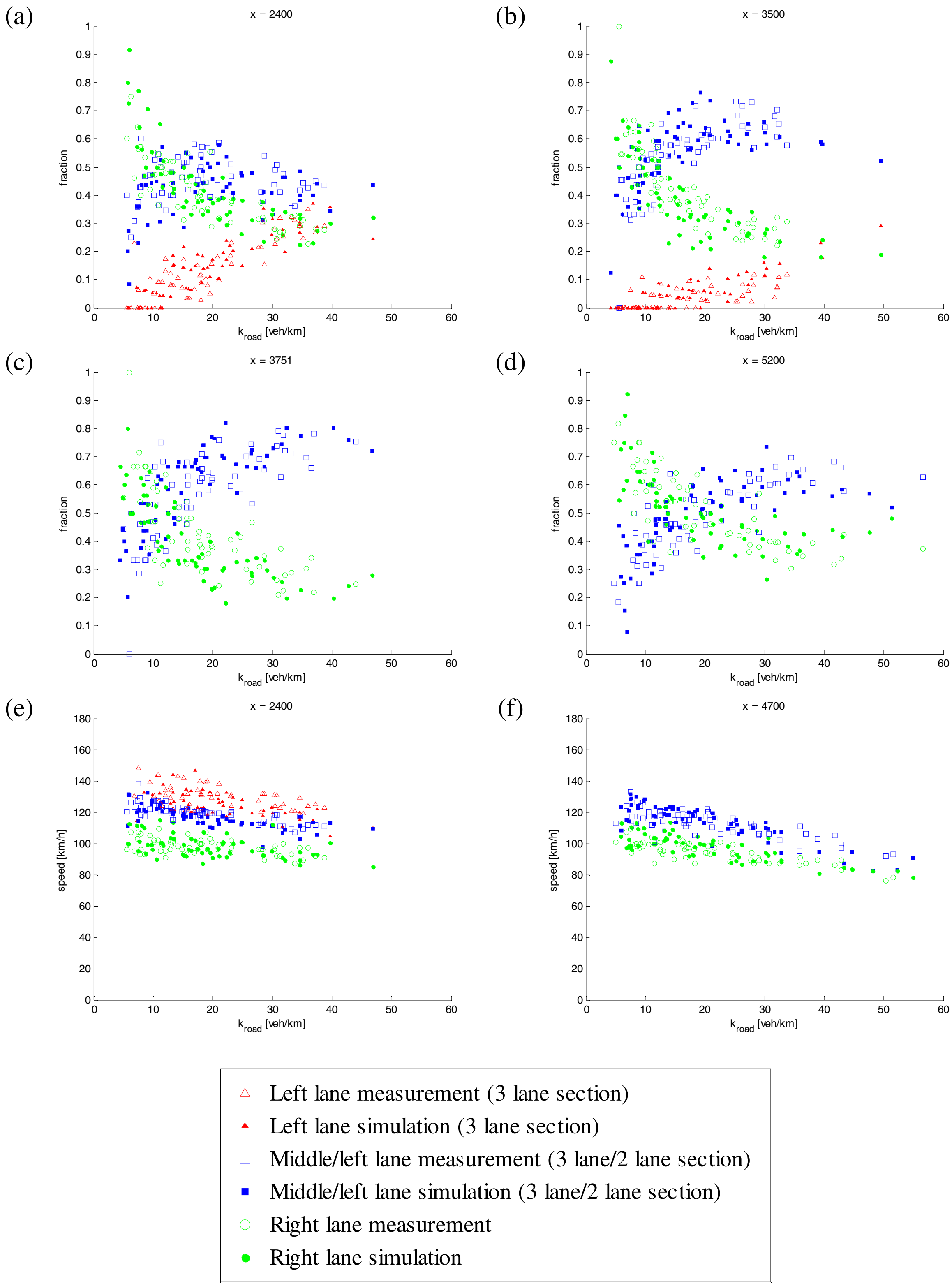

FIGURE 3 Calibrated lane fractions in free flow (run 1) at x = 2400m (a), x = 3500m (b), x = 3751m (c) and x = 5200m (d). Calibrated lane speeds in free flow (run 1) at x = 2400m (e) and x = 4700m (f). Each dot represents a 1-minute measurement.

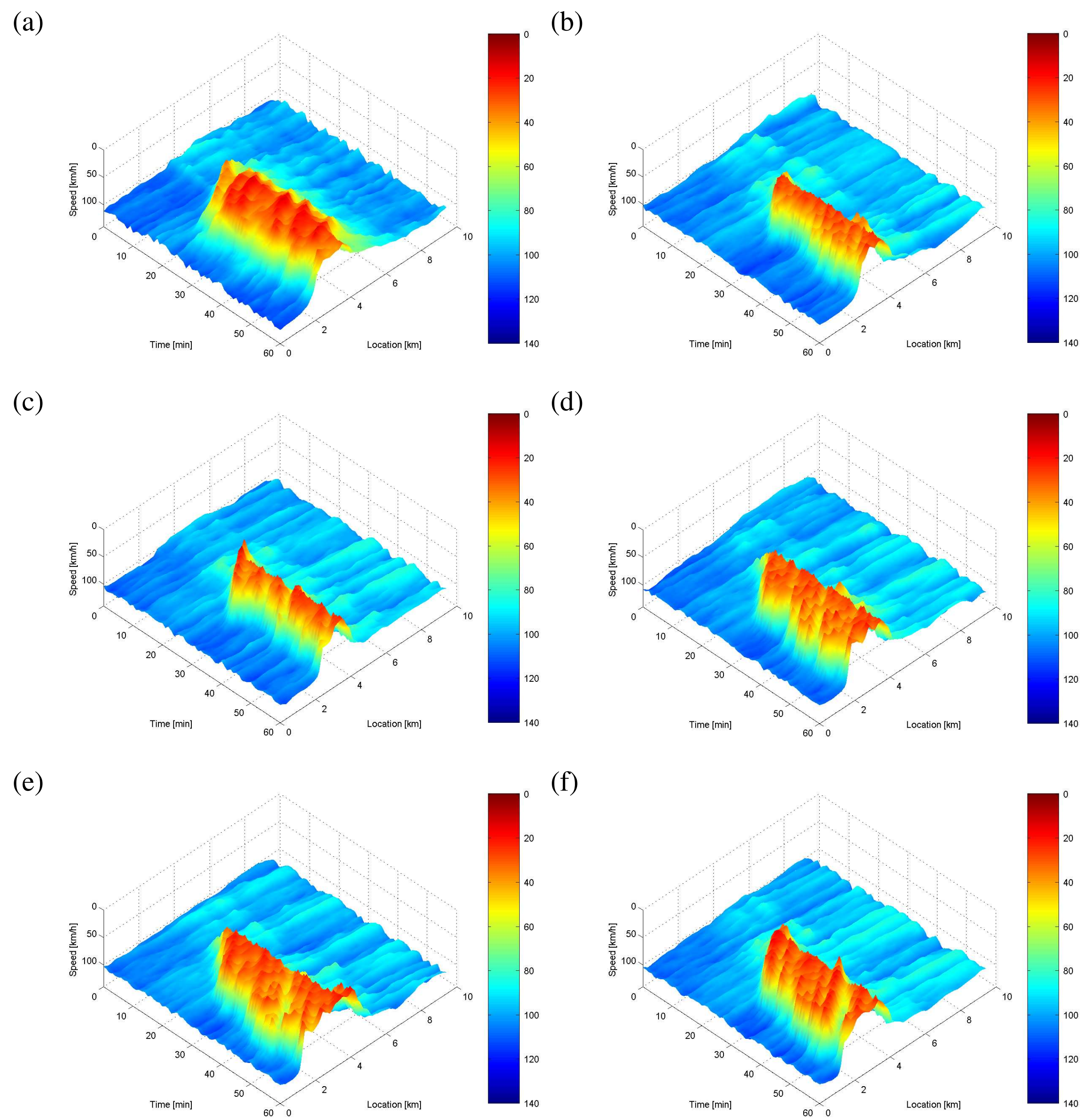

FIGURE 4 Speed pattern for the calibration day June 8th 2009 in the congestion scenario. Real data (a) and five model runs (b)-(f).

The model has been validated by running the model with data from June 25th 2009. It is difficult to compare the model fit based on the error as with more traffic the RMSE of flow will also increase for an equal error in terms of percentage. On June 25th there was 26% more traffic in the free flow scenario resulting in larger values of the RMSE of flow. This growth causes most of the increase of the total error in free flow. Keeping this in mind and looking at the RMSE of speed we can conclude that the model does not appear to have a significantly different fit to data in free flow.

Traffic demand in the congestion scenario differs by only 1.2% between both days, but still the underlying demand pattern can strongly influence the amount of congestion. Remarkably, the error value is smaller on the validation day even though the fit appears worse than the calibration, as the validation runs produce no congestion. In general we consider that the model is able to show a good fit to data. Validation results are reasonable given the large stochastic influence of driver behavior.

TABLE 2 Calibration and validation errors of the free flow and congestion scenario.

Day	Error measure	Error value
	Free flow scenario	
Monday June 8th 2009	RMSE flow [veh/h]	33.6
(calibration day)	RMSE speed [km/h]	4.70
	Total (ε_{free})	154.8
Thursday June 25th 2009	RMSE flow [veh/h]	61.4
	RMSE speed [km/h]	5.35
	Total (ε_{free})	202.4
	Congestion scenario	
Monday June 8th 2009	RMSE flow [veh/h]	440
(calibration day)	RMSE speed [km/h]	22.6
	Total (ε_{cong})	1011.6
Thursday June 25th 2009	RMSE flow [veh/h]	373
	RMSE speed [km/h]	19.8
	Total (ε_{cong})	877.5

A sensitivity analysis was also performed to verify whether the calibration method of using two scenarios was valid. Parameter values were changed from 50% to 150% of the original value while keeping all other parameters fixed to determine changes in the error. It appeared that parameters were significant in their respective scenarios. More importantly, they were not significant in a wide range around their initial value in the scenario where they were kept constant.

SUMMARY AND CONCLUSIONS

A lane change model has been proposed that is build around a lane change desire that follows from a combination of the route, speed and keep-right incentives. Within the combination of incentives there is a trade-off in which the route incentive becomes increasingly dominant. For an increasing level of lane change desire drivers become more assertive. For little desire, no lane change will be performed. For slightly more desire lane changes are only performed in a free fashion. For medium desire drivers will start to synchronize with the target lane and for high desire, the potential follower on the target lane is assumed to create a gap as it notices the lane change desire. The relaxation phenomenon is implemented as drivers accept smaller headways for larger desire.

The model has been calibrated and validated in both free flow and congested traffic conditions. In free flow, we get a good fit to lane distributions for different levels of density on a particular cross-section of the road. Speeds on the different lanes for different levels of density are also realistic. The fit in congestion is less clear as this highly depends on the stochastic input. For some runs we however find good fit on the location and moment of breakdown and the following progression of congestion. A sensitivity analysis shows that the approach of two calibration scenarios is appropriate.

The model is able to represent lane changing behavior with a set of 7 parameters that all have a physical and intuitive meaning. The model has been calibrated and validated to a section on the A20 highway. Future research should be aimed at investigating whether the model is generally applicable to other locations with different speed limits and more lanes. Also, the large speed threshold to change lane indicates speed adaptation behavior. A more elaborate model regarding speed adaptation could improve results.

ACKNOWLEDGEMENT

The research reported in this paper was conducted as part of the Connected Cruise Control project funded by the Dutch Ministry of Economic Affairs under the High Tech Automotive Systems program, by the universities of Delft, Twente and Eindhoven and NXP, NAVTEQ, TNO, Clifford, Technolution, Rijkswaterstaat and SWOV.

REFERENCES

[1] Gipps, P.G., “A Behavioral Car Following Model for Computer Simulation”, Transportation Research Part B, Vol. 15, Issue 2, 1981, pp. 105-111.

[2] Wiedemann R., "Simulation des Straßenverkehrsflusses", SChriftenreihe des Institutes für Verkehrswesen der Universität Karlsruhe, Heft 8, Karlsruhe, 1974.

[3] Bando, M., Hasebe, K., Nakayama, A., Shibata, A., Sugiyama, Y., “Dynamical model of raffic congestion and numerical simulation”, Physical Review E. 51, 1995, pp. 1035-1042.

[4] Tampère, C.M.J., “Human-kinetic multiclass traffic flow theory and modeling”, Ph.D. Thesis, TRAIL Thesis Series, 2004.

[5] Treiber, M., A. Hennecke, and D. Helbing, “Congested traffic states in empirical observations and microscopic simulations”, Physical Review E. 62, 2000, pp. 1805-1824.

[6] Kesting A., M. Treiber, and D. Helbing, “General Lane changing Model MOBIL for Car-Following Models”, Transportation Research Record: Journal of the Transportation Research Board, Vol. 1999, 2007, pp. 86-94.

[7] Laval, J.A., and C.F. Daganzo, “Lane changing in traffic streams”, Transportation Research Part B, Vol. 40, Issue 3, 2006, pp. 251-265.

[8] Gipps, P.G., “A model for the structure of lane changing decisions”, Transportation Research Part B, Vol. 20, Issue 5, 1986, pp. 403-414.

[9] Toledo, T., H.N. Koutsopoulos, and M . Ben-Akiva, “Integrated driving behavior modeling”, Transportation Research Part C, Vol. 15, Issue 2, 2007, pp. 96-112.

[10] Daamen, W., M. Loot, and S.P. Hoogendoorn, “Empirical Analysis of Merging Behavior at Freeway On-Ramp”, Transportation Research Record: Journal of the Transportation Research Board, Vol. 2188, 2010, pp. 108-118.

[11] Laval, J.A., and L. Leclercq, “Microscopic Modeling of the Relaxation Phenomenon Using a Macroscopic Lane changing Model”, Transportation Research Part B, Vol. 42, 2008, pp. 511-522.

[12] Smith, S.A., “Freeway Data Collection for Studying Vehicle Interaction”, Technical report. FHWA/RD-85/108. FHWA, U.S. Department of Transportation, 1985.

[13] Sultan, B., M. Brackstone, B. Waterson, and E.R. Boer, “Modeling the Dynamic Cut-In Situation”, Transportation Research Record: Journal of the Transportation Research Board, Vol. 1803, 2002, pp. 45-51.

[14] Wang, J., R. Liu, and F. Montgomery, “A Simulation Model for Motorway Merging Behavior”, 16th International Symposium on Transportation and Traffic Theory (H. S. Mahmassani, ed.), 2005, pp. 281-301.

[15] Hidas, P., “Modelling lane changing and merging in microscopic traffic simulation”, Transportation Research Part C, Vol. 10, 2002, pp. 351-371.

[16] Cohen, S.L., “Application of Relaxation Procedure for Lane Changing in Microscopic Simulation Models”, Transportation Research Record: Journal of the Transportation Research Board, Vol. 1883, 2004, pp. 50-58.

[17] Yeo H., A. Skabardonis, J. Halkias, J. Colyar, and V. Alexiadis, “Oversaturated Freeway Flow Algorithm for Use in Next Generation Simulation”, Transportation Research Record: Journal of the Transportation Research Board, Vol. 2088, 2008, pp. 68-79.

[18] Choudhury C., M. Ben-Akiva, T. Toledo, G. Lee and A. Rao, “Modeling Cooperative Lane changing and Forced Merging Behavior”, Transportation Research Board Annual Meeting, January 2007.

[19] Dijker, T., and P. Knoppers, FOSIM 5.0 Gebruikershandleiding, FOSIM 5.0 User manual, 2004, www.fosim.nl

[20] Daganzo, C.F., “A behavioral theory of multi-lane traffic flow. Part I: Long homogeneous freeway sections”, Transportation Research Part B, Vol. 36, Issue 2, February 2002, pp. 131-158.

[21] Schakel, W.J., B. van Arem, and B. Netten, “Effects of Cooperative Adaptive Cruise Control on Traffic Flow Stability”, Proceedings of the 13th International IEEE Conference on Intelligent Transportation Systems (ITSC 2010), 2010, pp. 759-764.

[22] Ossen, S. and S.P. Hoogendoorn, “Reliability of parameter values estimated using trajectory observations”, Transportation Research Record: Journal of the Transportation Research Board, Vol. 2124, 2009, pp. 36-44.

[23] Hoogendoorn, S.P., H.J. van Zuylen, M. Schreuder, B.G.H. Gorte, and G. Vosselman, “Microscopic Traffic Data Collection by Remote Sensing”, Transportation Research Record: Journal of the Transportation Research Board, Vol. 1855, 2003, pp. 121-128.

[24] Treiber, M., and D. Helbing, “An adaptive smoothing method for traffic state identification from incomplete information”, in: H. Emmerich, B. Nestler, and M. Schreckenberg (eds.) Interface and Transport Dynamics. Computational Modelling, Springer, Berlin, 2003, pp. 343-360.